Draft version August 28, 2012
Preprint typeset using LaTeX style emulateapj v. 5/2/11

arXiv:1208.5069v1 [astro-ph.HE] 24 Aug 2012

FAILED-DETONATION SUPERNOVAE: SUB-LUMINOUS LOW-VELOCITY IA SUPERNOVAE AND THEIR REMNANT-KICKED IRON-CORE WHITE DWARFS

George C. Jordan IV,[1,2] Hagai B. Perets,[3,4] Robert T. Fisher[5] Daniel R. van Rossum,[1,2]

Draft version August 28, 2012

ABSTRACT

Type Ia supernovae (SNe Ia) are thought to originate from the thermonuclear explosions of carbon-oxygen (C-O) white dwarfs (WDs). The gravitationally-confined detonation (GCD) model is a well-explored explosion model where unstable thermonuclear burning initiates in an accreting, Chandrasekhar-mass WD and forms an advancing flame. Rising, burning material breaks out of the WD surface, engulfs the WD, and leads to a gradient-induced detonation in the collision region, which subsequently unbinds the WD. We show that when the flame consumes enough fuel, the conditions for detonation are not met, and the WD does not detonate. We show through 2D and 3D simulations, such failed-detonation SNe expel a few 0.1 $M_\odot$ of burned and partially-burned material, but do not unbind the WD. A fraction of the material falls back onto the WD, polluting the remnant WD with intermediate-mass and iron-group elements, that likely segregate to the core forming an iron-core C-O WD. The remaining material is asymmetrically ejected at velocities comparable to the escape velocity from the WD, and in response, the WD is kicked to velocities of a few hundred km s^{-1}. Such kicks may unbind the binary and eject a runaway/hyper-velocity WD. Although the energy and ejected mass of the failed-detonation SN are a fraction of typical thermonuclear SNe, they are likely to appear as sub-luminous low-velocity SNe Ia. Such failed-GCDs might therefore explain or are related to the observed branch of peculiar SNe Ia, such as the family of low-velocity sub-luminous SNe (SN 2002cx/SN 2008ha-like SNe).

Subject headings: supernovae: general — supernovae: individual (2002cx, 2008ha) — hydrodynamics — white dwarfs — ISM: supernova remnants

1. INTRODUCTION

Type Ia supernovae (SNe Ia) are among the most energetic explosions in the known universe, releasing $\sim 10^{51}$ ergs of kinetic energy in their ejecta, and synthesizing $\sim 0.7\ M_\odot$ of radioactive ^{56}Ni. The discovery of the Phillips relation (Phillips 1993) enabled the use of SNe Ia as standardizable cosmological candles, and has ushered in a new era of astronomy leading to the discovery of the acceleration of the universe (Riess et al. 1998; Perlmutter et al. 1999), leading to the 2011 Nobel Prize in physics.

In the following we introduce an unexplored variant of well-studied single-degenerate (SD) model of SNe Ia in which a Chandrasekhar-mass, carbon-oxygen (C-O) WD accretes mass from a non-degenerate main sequence or red giant companion. As the WD approaches the Chandrasekhar limit, carbon burning is initiated in its convective core. After a few hundred years of this "simmering" phase, unstable thermonuclear burning is expected to ignite at one or more off-centered points, generating a buoyantly-rising, subsonic deflagration flame bubble (Kuhlen et al. 2006; Zingale et al. 2009, 2011). We refer to this phase as the "deflagration phase".

We adopt the assumption made by the gravitationally-confined detonation (GCD) scenario (Jordan et al. 2008; Meakin et al. 2009; Jordan et al. 2012) of SNe Ia in which no transition to detonation occurs as the rising flame approaches the low-density surface layers of the WD as is posited by the "deflagration-to-detonation transition" (DDT) model of SNe Ia (Khokhlov 1991; Gamezo et al. 2004, 2005). We assume an off-centered distribution of ignition points as in the GCD scenario. We further focus on the "pulsationally-assisted" variant of the GCD model described in Jordan et al. (2009, 2012) which we review in section 2.

We demonstrate that under these assumptions, if enough mass is burned during the deflagration phase, the conditions to trigger a detonation via the GCD mechanism are not realized and the WD *fails to detonate*. Such "failed-detonation" (FGCD) models have numerous remarkable implications for the observable properties of the resulting explosion and its outcomes. These include the production of peculiar SNe Ia events with low expansion velocities, low luminosities and low ejecta-mass; all broadly consistent with the observed properties of a branch of peculiar SNe Iasimilar to SN 2002cx and/or SN 2008ha. Even more remarkably, we demonstrate that the WD survives the initial Ia event, receiving a large velocity kick from the asymmetric nature of the initial deflagration, and is significantly enriched with both intermediate-mass (IME's) and iron-group elements (IGE's), forming a peculiar heavy/iron core WD.

2. PHYSICS OF THE FAILED-DETONATION SCENARIO

The pulsationally-assisted GCD model described in Jordan et al. (2012) begins with an off-centered ignition

[1] Center for Astrophysical Thermonuclear Flashes, The University of Chicago, Chicago, IL 60637.
[2] Department of Astronomy and Astrophysics, The University of Chicago, Chicago, IL 60637.
[3] Harvard-Smithsonian Center for Astrophysics, 60 Garden St., Cambridge, USA 02138
[4] Physics department, Technion - Israel Institute of Technology, Haifa, Israel 32000.
[5] University of Massachusetts Dartmouth, Department of Physics, 285 Old Westport Road, North Dartmouth, 02740.

region in a Chandrasekhar-mass WD which forms an advancing thermonuclear flame. The hot, buoyant ash quickly rises forming a large plume that advances and burns towards the surface of the star. Energy imparted to the WD during the deflagration causes the star to pulse. As the WD expands, hot ash erupts from the star, flows around the stellar surface, and mixes with cold fuel. The mixture collides at the antipodal point on the surface from breakout. Meanwhile, the WD reaches maximum expansion and contracts. As the star contracts, it squeezes the fuel-ash mixture in the collision region to temperatures and densities that considerably shorten the minimum length scale on which the Zel'dovich gradient mechanism can trigger a detonation. A detonation is triggered in the mixture which subsequently consumes the WD.

Roughly speaking, typical fuel-ash mixture properties associated with an induction gradient $\lesssim 10$ km are densities $\gtrsim 1\times10^7$ g/cm^3 and peak temperatures $\gtrsim 1\times10^9$ K (see Arnett & Livne 1994; Niemeyer & Woosley 1997; Khokhlov et al. 1997; Röpke et al. 2007; Seitenzahl et al. 2009a, for a complete discussion).

The FGCD scenario proceeds similarly to the pulsational GCD model; however, the scenarios deviate in the amount of burning — and therefore the amount of energy released — during the deflagration phase. More burning occurs during the deflagration phase of the FGCD than in the GCD which means more mass is consumed by the flame and ejected from the star in the form of ash, and more energy is delivered to the WD. The WD is thus modified to a higher degree than in the GCD model and as a result, the WD does not attain high densities and temperatures in the collision region during its contraction. The fuel-ash mixture never reaches the critical conditions for detonation and therefore *the star never detonates.*

The deflagration is strong enough to prevent the formation of the conditions for detonation, but too weak to completely unbind the star. The WD will thus remain intact; though, it will have a lower mass. Interestingly, since the ignition of the deflagration is off-centered, the remaining bound stellar material is kicked by the ejection of the ash and obtains a velocity of hundreds of km s^{-1}.

This system produces an asymmetric outburst of a few tenths of a solar mass of deflagration products rich in IME's (such as Mg, Si, and S) and iron-group elements IGE's (such as Fe, Co, and Ni). Since the deflagration only processes a few tenths of a solar mass of material, the FGCD produces a small total mass of ^{56}Ni compared to normal SNe Ia which convert nearly half of the WD to ^{56}Ni.

Some of this material attains escape velocity and some falls back onto the star. The velocity of the outflow will be slow (approximately a few thousand km s^{-1}) related to normal SNe Ia due to the comparatively small amount of energy released in the FGCD scenario.

3. SIMULATIONS OF THE FGCD MODEL

3.1. *Simulation Setup*

We used the Adaptive Mesh Refinement (AMR) FLASH application framework (Dubey et al. 2009; Fryxell et al. 2000) to perform our simulations of FGCD models. FLASH has been previously used to simulate SNe Ia in both 2D cylindrical and 3D Cartesian geometry (Jordan et al. 2012, 2008; Meakin et al. 2009). Our simulations include an advection-diffusion-reaction (ADR) treatment of the thermonuclear flame (Calder et al. 2007; Townsley et al. 2007; Seitenzahl et al. 2009b), an equation of state that includes contributions from blackbody radiation, ions, and electrons of an arbitrary degree of degeneracy (Timmes & Swesty 2000), and the multipole treatment of gravity included in the FLASH standard (ASC FLASH Center 2012).

We performed four 3-dimensional (3D) exploratory simulations to test the feasibility of the FGCD and 1 full 2-dimensional (2D) model to adequately observe the FGCD at late times.

Our 3D simulations included a reduced domain size and a moderate resolution (8 km) which reduced their computational expense. We initialized these simulations similarly to those in Jordan et al. (2012) with a 1.365 $M_\odot$ WD placed at the origin of the domain. We used the same distribution of sixty three, 16 km radius ignition "points" distributed in a 128 km radius spherical volume. We chose 48 km, 38, km, 28 km, and 18 km as offset distances along the z-axis of the spherical volume. Table 1 lists the initial conditions for each simulation and the corresponding names we gave them. We ran the simulations from ignition, through peak stellar expansion, and at least until the WD reached a maximum central density upon contraction.

Our 2D simulation was performed with a large domain in 2D cylindrical geometry at 4 km resolution and ran for 60 seconds. This simulation was initialized similarly to the 3D simulations except we placed only 4 bubbles in a 64 km spherical volume offset by 70 km along the z-axis (axis of symmetry). We chose these initial conditions to obtain an FGCD in 2D given what we learned from our 3D simulations. The larger domain size allowed us to follow the outer layers of the ejecta for the entirety of the simulation.

3.2. *Simulation Results*

We obtained an FGCD from each of our simulations. and were able to quantify features discussed in section 2. Table 1 contains a collection of these quantities from our simulations.

The energy liberated during the deflagration is between 89% and 150% of the binding energy of the WD. However, in each simulation the deflagration fails to unbind the WD. The WD expands in response to the deflagration, reaches its maximum level of expansion, and then contracts. Figure 1 shows the evolution of the central density, ρ_c, of the WD and illustrates the oscillatory nature of the WD after the deflagration. The more energy released during the deflagration, the more the star expanded, the longer the pulsational period, and the smaller the ρ_c at maximum contraction.

The fact that the deflagration releases more than 100% WD binding energy in some models suggests that the WD should be unbound after the deflagration; however, the entire energy budget does not work to only unbind the star. For example, some of the energy is lost when the ejecta and the remnant WD are accelerated to high velocities. Thus, even though the deflagration liberates enough energy to completely unbind the star, the energy

TABLE 1
Simulations Properties

sim name	Δx[a] (km)	$\mathrm{n_{ign}}$[b]	$\mathrm{r_{ign}}$[c] (km)	$\mathrm{z_{ign}}$[d] (km)	$\mathrm{E_{nuc}}$[e] (E_{bin})	C-$\mathrm{O_B}$[f] ($M_\odot$)	$\mathrm{IME_B}$ ($M_\odot$)	$\mathrm{IGE_B}$ ($M_\odot$)	$\mathrm{v_B}$[g] (km $\mathrm{s^{-1}}$)	C-$\mathrm{O_E}$[h] ($M_\odot$)	$\mathrm{IME_E}$ ($M_\odot$)	$\mathrm{IGE_E}$ ($M_\odot$)	$\mathrm{E_{kin,E}}$[i] (ergs $\cdot 10^{50}$)	$\mathrm{v_{ave,E}}$ (km s
2D70	4	4	64.0	70.0	0.89	0.93	0.07	0.13	119	0.13	0.03	0.07	0.32	3,730
3D48	8	63	128.0	48.0	1.06	0.84	0.06	0.09	351	0.16	0.05	0.16	0.90	4,932
3D38	8	63	128.0	38.0	1.21	0.71	0.07	0.08	383	0.24	0.06	0.20	1.3	5,099
3D28	8	63	128.0	28.0	1.39	0.56	0.05	0.09	520	0.32	0.09	0.25	1.8	5,222
3D18	8	63	128.0	18.0	1.53	0.43	0.04	0.08	406	0.43	0.10	0.28	2.2	5,212

[a] Maximum spatial resolution.
[b] Number of ignition points.
[c] Radius of the spherical volume containing the ignition points.
[d] Z coordinate of the origin of the spherical volume containing the ignition points.
[e] Energy released during the deflagration phase divided by the binding energy of the star ($E_{bin} = 4.5 \times 10^{50}$ ergs).
[f] "B" refers to gravitationally bound material.
[g] Velocity of the gravitationally bound material .
[h] "E" refers to material that will escape the system.
[i] Average kinetic energy of the escaping material.
[j] Mass weighted velocity of escaping material.

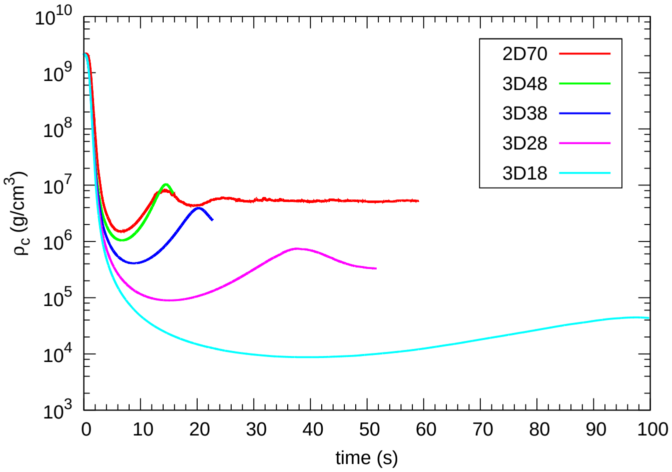

Fig. 1.— The central density, ρ_c, of the WD vs time. Note that the ρ_c achieved during contraction is $\lesssim 10^7$ g/cm^3, the density at which the Zel'dovich gradient mechanism can produce a detonation on length scales less than ~ 10 km.

is partitioned in such a way that a portion of the original WD remains gravitationally bound.

In each of our models, the WD gets a kick in the opposite direction from which the buoyant ash rises and breaks through the surface of the star. We measured this velocity to be on the order of hundreds of km s^{-1}and list these values for each simulation in table 1.

Some of the material from the FGCD escapes and achieves high velocities, while some of the material is bound to the remnant WD and will eventually accrete onto its surface. Table 1 lists the composition of material that remains gravitationally bound and eventually will mix with the remnant WD. In all cases between 0.1 $M_\odot$ and 0.2 $M_\odot$ of IME's and IGE's (some of which is radioactive ^{56}Ni) remained bound to the star. The evolution of the WD as the material falls back onto and heats the star is an interesting question and one which we will examine in future work.

The composition of the material that escapes the system is also listed in table 1 along with the kinetic energy and the mass-weighted velocity of the ejecta. This material includes carbon and oxygen, IME's, and IGE's, and ranges from 0.2 to 0.8 $M_\odot$. In general, the more material that is burned during the deflagration, the more material that escapes.

Figure 2 shows shows the density structure and composition with overlaid velocity contours of the 2D model at 60s. Note that the density profile of the FGCD model is asymmetric in velocity space between the hemisphere corresponding to the ejected deflagration and the opposite hemisphere of the system. The remnant of the WD can be seen as the tiny high-density feature slightly below the origin of the domain.

The figure also shows the nature of the asymmetry in composition of the structure. The north side of the remnant contains the products of the deflagration that were sprayed from the surface of the WD. Clumpy structures of IME's and IGE's exist at a range of velocities in the northern hemisphere of the domain but are less abundant in the southern hemisphere. The asymmetries suggest that this object would look much different depending on the viewing angle of the observer.

All of our models produce a relatively small amount of radioactive ^{56}Ni. Though we do not perform detailed nucleosynthetic post processing of the 3D models, we can set an upper limit on the ^{56}Ni yields with the amount of IGE's produced, which ranges from 0.2 $M_\odot$ to 0.36 $M_\odot$. Neutronization through electron capture reactions during the deflagration would shift production away from ^{56}Ni though and reduce its contribution to the IGE totals. Whether even lower masses of IGE's (and thus ^{56}Ni) could be produced under appropriate conditions (e.g. comparable to that observed in SN 2008ha, a very faint SN with extremely low ejecta velocities), is yet to be explored.

4. DISCUSSION AND PREDICTIONS

4.1. *Sub-luminous Low-Velocity SNe*

The most prominent features of the FGCD models are their low-mass, low-velocity ejecta and overall low kinetic and nuclear energy. These properties translate into the production of typically sub-luminous, low-velocity SNe Ia. It is therefore natural to examine whether SNe with such characteristics have already been discovered. In particular, one may explore peculiar SNe exhibiting either extremely low mass ejecta, such as SN 2008ha

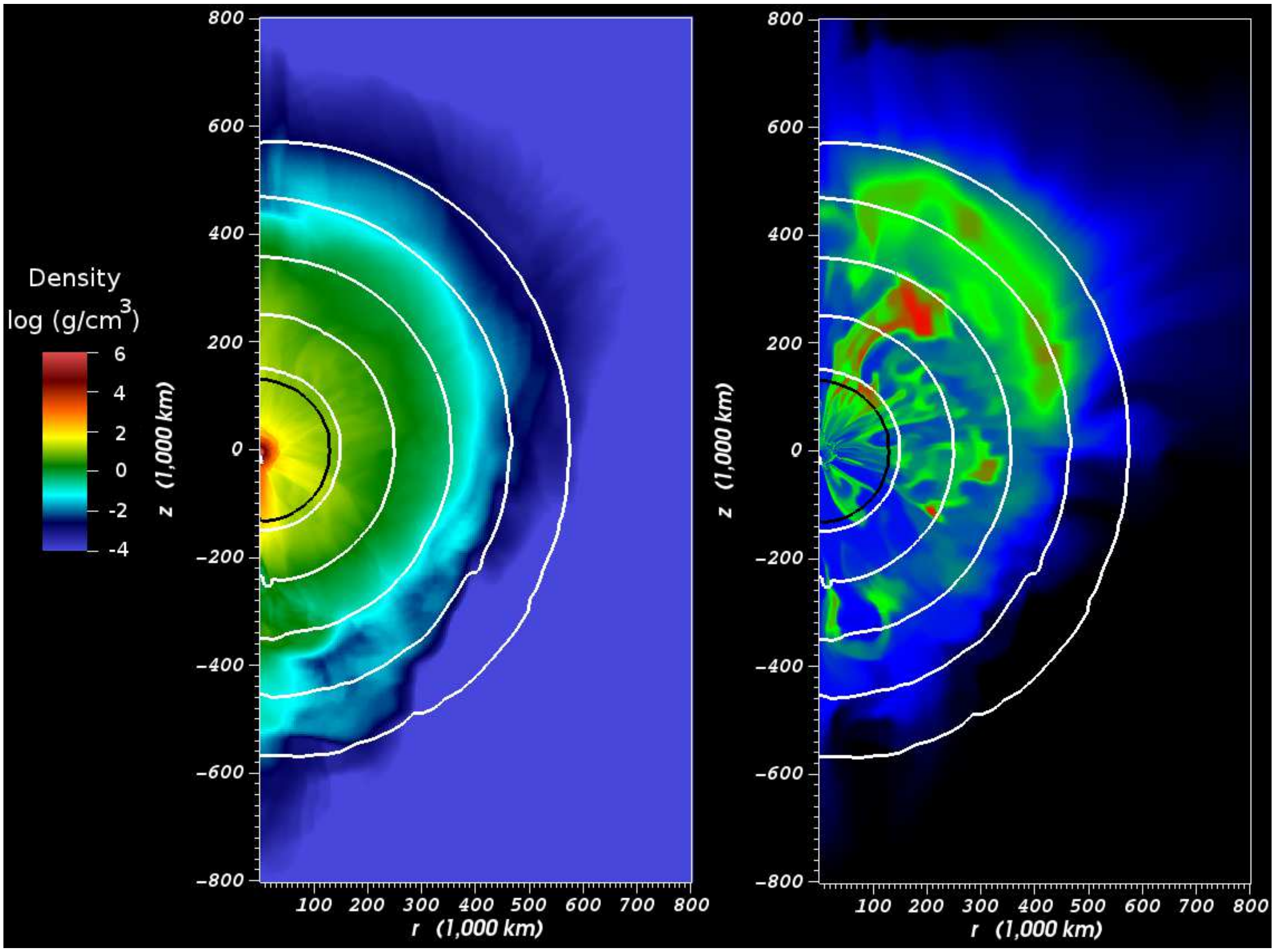

FIG. 2.— Images from the $2D70$ simulation. The black contour marks the transition between gravitationally bound and escaping material. The white contours are of the magnitude of the velocity field. From the inner most contour and moving outwards, the values are: 2,000 km s^{-1}, 4,000 km s^{-1}, 6,000 km s^{-1}, 8,000 km s^{-1}, and 10,000 km s^{-1}. The images show the simulation at 60 seconds. (*left*) Log density of the remnant. The values of the density are given by the color bar on the left. (*right*) The composition of the remnant. Blue is C-O, green is IME's, and red is IGE's.

(Foley et al. 2009; Valenti et al. 2009), SN 2005E-like SNe (Perets et al. 2010; Kasliwal et al. 2012a), or SN 2002bj-like SNe (Kasliwal et al. 2012b; Poznanski et al. 2010; Perets et al. 2011), or low ejecta velocity such as SN 2002cx-like SNe Li et al. (2003); Branch et al. (2004); Jha et al. (2006). Some of the former low-mass-ejecta SNe, however, may present He signature in their spectra (type Ib SNe), inconsistent with our models. We therefore focus on observed low velocity, faint SNe Ia.

Normal type Ia SNe differ in their ejecta velocities as measured in some standard method, but they generally fall between $9000 - 14000$ km s^{-1} near peak luminosity, with similar dispersion at later times (as derived from the Si II line Bender et al. 2005). The velocities of even the lowest velocity SNe in the Bender et al. (2005) sample much exceed the mass-averaged FGCD velocities listed in table 1. We also note a trend of more energetic and likely more luminous (larger IGE yield) SNe to be accompanied by higher ejecta-velocities over almost an order of magnitude in kinetic energy. The only other type of SNe with such low expansion velocities are the branch of peculiar type Ia SNe, named for the prototype for this class of supernovae, 2002cx (Li et al. 2003; Branch et al. 2004; Jha et al. 2006); such SNe may also have an enregy-velocity correlation McClelland et al. (2010) as observed in our simulations.

SN 2002cx-like events are characterized by luminosities which lie too low in comparison to the Phillips relation for Branch-normal Ia events (Li et al. 2003), low photospheric velocities (Li et al. 2003), weak intermediate-mass element lines (including Si II, S II, Si III, and Ca II) (Branch et al. 2004), and late-time optical nebular spectra dominated by narrow Fe II lines (Branch et al. 2004; Jha et al. 2006). Since the discovery of SN 2002cx, a number of other 2002cx-like events have been discovered, including 2002es, 2005P, 2005hk (Chornock et al. 2006), 2008ge (Foley et al. 2010a) and 2008ha. The latter event (SN 2008ha), in particular, is consistent with extremely low mass ejecta and energetics. We predict the FGCD models to produce similar properties to those characterizing SN 2002cx like SNe, given the low expansion velocities and the low estimated ^{56}Ni yield, and potentially even explaining SN 2008ha like events with low mass ejecta.

Though our initial set of simulations is limited, the robust features of FGCD's, including low velocity ejecta, the expected low luminosity (due to the small yield of ^{56}Ni) and their low mass ejecta (comparable to that SN 2008ha) make them tantalizing candidate progenitors for this branch of peculiar SNe. Note that the single degenerate origin of such SNe is also consistent with the overall typically young (but not *necessarily* young; Foley et al. 2010) environments found for SN-2002cx like SNe, compared to the expectations from, e.g. double degenerate SNe (older environments) or core-collapse SNe (only very young environments).

4.2. *Heavy metal/Iron-core WD*

In our FGCD scenario, a large amount of burnt material falls back to the remnant WD. From table 1, the WD may incorporate as much as 0.1 $M_\odot$ of IGE's and 0.07 $M_\odot$ of IME's of fallback material, together comprising as much as $\sim 1/4$ of the remnant C-O WD. Such heavy elements are likely to gravitationally settle, in time, to the WD core, making these heavy-metal polluted WD's become iron/heavy-core WDs. The existence of iron-core WD's has been considered before, with even the potential observation of such WDs (Provencal et al. 1998; Catalán et al. 2008). The FGCD scenario therefore provides a novel evolutionary scenario for the formation of these iron/heavy-core C-O WD's. A somewhat related scenario of failed SN was suggested for the formation of O-Ne-Mg WDs with iron cores (Isern et al. 1991).

4.3. *WD Natal Kicks*

FGCD's produce a highly asymmetric ejection of material. This is not unique amongst various models for SNe explosions. However, in our FGCD case, the WD survives the explosion. Considering momentum conservation, this gives rise to a unique outcome, namely that the surviving WD is kicked at very high velocities, ranging hundreds of km s^{-1}. The FGCD scenario suggests the existence of strong WD natal kicks, and provides an interesting prediction per the existence of hypervelocity WDs. Taken together, the potential existence of a a heavy core WD (discussed in section 4.2), and the high ejection velocity produce a highly peculiar object, which, if observed may provide a possibly unique smoking gun signature. One should note, however, that the population of halo WDs may also have relatively high velocities, and it might therefore be difficult to pinpoint the kinematic property as related to a natal kick (unless the WD is massive and young; an unlikely possibility for the old population of halo WDs).

We note that velocities of hundreds of km s^{-1} are much larger than the orbital velocities of most binaries, and a kick velocity of such magnitude is likely to unbind the binary (ejecting the companion star at high velocity, but much lower than the WD kick velocity). WD's accreting from evolved stars could have a large binary separation, and be disrupted following the WD kick. However, WD's accreting from a main sequence companion might have highly compact configurations. In this latter case, the WD kick might not unbind the binary, and may only change its orbit, and provide an overall kick to the binary center of mass as a whole. An interesting aspect is then the result of a following accretion epoch involving the iron-core WD, and its possible evolutionary outcomes. Finally, in both cases of evolved and main sequence mass donors, the WD natal kick may eject the remnant WD towards the companion, in which case a collision may occur, with potentially interesting explosive results.

5. SUMMARY

We have discovered a scenario in which the standard GCD model fails to detonate due to a large amount of burning during the deflagration phase. The failed GCD results in an asymmetric outburst of deflagration material consisting of intermediate elements and iron group elements along with a fraction of the original WD still gravitationally bound. The models produce a faint SNe Ia with a slowly evolving light curve due to the low ^{56}Ni yield and the low energetics. The remaining WD gets a kick on the order of hundreds of km s^{-1} and is contaminated with fall-back from the deflagration, producing an iron/heavy core WD. We presented our initial simulations to quantify the some of the bulk observable properties and hypothesize that the FGCD model is a possible explanation for 2002cx-like SN. Future studies will explore the detailed observational features of FGCD SNe and their direct comparison to observations.

The authors thank the FLASH Code Group, the FLASH Astrophysics Group, and the Argonne Leadership Computing Facility at Argonne National Laboratory. HBP is supported by the CfA and BIKURA prize fellowships. This work was supported in part at the University of Chicago by the U.S Department of Energy (DOE) under Contract B523820 to the ASC Alliances Center for Astrophysical Nuclear Flashes, and in part by the National Science Foundation under Grant No. AST - 0909132 for the "Petascale Computing of Thermonuclear Supernova Explosions". This research used computational resources awarded under the INCITE program at ALCF at ANL, which is supported by the Office of Science of the US Department of Energy under Contract No. DE-AC02-06CH11357.

REFERENCES

Arnett, D. & Livne, E. 1994, ApJ, 427, 330

ASC FLASH Center. 2012, FLASH User's Guide, 4th edn., University of Chicago, http://flash.uchicago.edu/website/codesupport/flash4_ug/

Bender, R. et al. 2005, ApJ, 631, 280

Branch, D., Baron, E., Thomas, R. C., Kasen, D., Li, W., & Filippenko, A. V. 2004, PASP, 116, 903

Calder, A. C., Townsley, D. M., Seitenzahl, I. R., Peng, F., Messer, O. E. B., Vladimirova, N., Brown, E. F., Truran, J. W., & Lamb, D. Q. 2007, ApJ, 656, 313

Catalán, S., Ribas, I., Isern, J., & García-Berro, E. 2008, A&A, 477, 901

Chornock, R., Filippenko, A. V., Branch, D., Foley, R. J., Jha, S., & Li, W. 2006, PASP, 118, 722

Dubey, A., Antypas, K., Ganapathy, M., Reid, L., Riley, K., Sheeler, D., Siegel, A., & Weide, K. 2009, Parallel Computing, 35, 512

Foley, R. J., Chornock, R., Filippenko, A. V., Ganeshalingam, M., Kirshner, R. P., Li, W., Cenko, S. B., Challis, P., Friedman, A. S., Modjaz, M., & Wood-Vasey, W. M. 2009, arXiv:0902.2794

Foley, R. J., Rest, A., Stritzinger, M., Pignata, G., Anderson, J. P., Hamuy, M., Morrell, N. I., Phillips, M. M., & Salgado, F. 2010a, AJ, 140, 1321

—. 2010b, AJ, 140, 1321

Fryxell, B., Olson, K., Ricker, P., Timmes, F. X., Zingale, M., Lamb, D. Q., MacNeice, P., Rosner, R., Truran, J. W., & Tufo, H. 2000, ApJS, 131, 273

Gamezo, V. N., Khokhlov, A. M., & Oran, E. S. 2004, Physical Review Letters, 92, 211102

—. 2005, ApJ, 623, 337

Isern, J., Canal, R., & Labay, J. 1991, ApJ, 372, L83

Jha, S., Branch, D., Chornock, R., Foley, R. J., Li, W., Swift, B. J., Casebeer, D., & Filippenko, A. V. 2006, AJ, 132, 189

Jordan, G. C., Meakin, C. A., Hearn, N., Fisher, R. T., Townsley, D. M., Lamb, D. Q., & Truran, J. W. 2009, in Astronomical Society of the Pacific Conference Series, Vol. 406, Astronomical Society of the Pacific Conference Series, ed. N. V. Pogorelov, E. Audit, P. Colella, & G. P. Zank, 92–+

Jordan, IV, G. C., Fisher, R. T., Townsley, D. M., Calder, A. C., Graziani, C., Asida, S., Lamb, D. Q., & Truran, J. W. 2008, ApJ, 681, 1448

Jordan, IV, G. C., Graziani, C., Fisher, R. T., Townsley, D. M., Meakin, C., Weide, K., Reid, L. B., Norris, J., Hudson, R., & Lamb, D. Q. 2012, ArXiv e-prints

Kasliwal, M. M., Kulkarni, S. R., Gal-Yam, A., Nugent, P. E., Sullivan, M., Bildsten, L., Yaron, O., Perets, H. B., Arcavi, I., Ben-Ami, S., Bhalerao, V. B., Bloom, J. S., Cenko, S. B., Filippenko, A. V., Frail, D. A., Ganeshalingam, M., Horesh, A., Howell, D. A., Law, N. M., Leonard, D. C., Li, W., Ofek, E. O., Polishook, D., Poznanski, D., Quimby, R. M., Silverman, J. M., Sternberg, A., & Xu, D. 2012a, ApJ, 755, 161

—. 2012b, ApJ, 755, 161

Khokhlov, A. M. 1991, A&A, 245, 114

Khokhlov, A. M., Oran, E. S., & Wheeler, J. C. 1997, ApJ, 478, 678

Kuhlen, M., Woosley, S. E., & Glatzmaier, G. A. 2006, ApJ, 640, 407

Li, W., Filippenko, A. V., Chornock, R., Berger, E., Berlind, P., Calkins, M. L., Challis, P., Fassnacht, C., Jha, S., Kirshner, R. P., Matheson, T., Sargent, W. L. W., Simcoe, R. A., Smith, G. H., & Squires, G. 2003, PASP, 115, 453

McClelland, C. M., Garnavich, P. M., Galbany, L., Miquel, R., Foley, R. J., Filippenko, A. V., Bassett, B., Wheeler, J. C., Goobar, A., Jha, S. W., Sako, M., Frieman, J. A., Sollerman, J., Vinko, J., & Schneider, D. P. 2010, ApJ, 720, 704

Meakin, C. A., Seitenzahl, I., Townsley, D., Jordan, G. C., Truran, J., & Lamb, D. 2009, ApJ, 693, 1188

Niemeyer, J. C. & Woosley, S. E. 1997, ApJ, 475, 740

Perets, H. B., Badenes, C., Arcavi, I., Simon, J. D., & Gal-yam, A. 2011, ApJ, 730, 89

Perets, H. B., Gal-Yam, A., Mazzali, P. A., Arnett, D., Kagan, D., Filippenko, A. V., Li, W., Arcavi, I., Cenko, S. B., Fox, D. B., Leonard, D. C., Moon, D.-S., Sand, D. J., Soderberg, A. M., Anderson, J. P., James, P. A., Foley, R. J., Ganeshalingam, M., Ofek, E. O., Bildsten, L., Nelemans, G., Shen, K. J., Weinberg, N. N., Metzger, B. D., Piro, A. L., Quataert, E., Kiewe, M., & Poznanski, D. 2010, Nature, 465, 322

Perlmutter, S., Aldering, G., Goldhaber, G., Knop, R. A., Nugent, P., Castro, P. G., Deustua, S., Fabbro, S., Goobar, A., Groom, D. E., Hook, I. M., Kim, A. G., Kim, M. Y., Lee, J. C., Nunes, N. J., Pain, R., Pennypacker, C. R., Quimby, R., Lidman, C., Ellis, R. S., Irwin, M., McMahon, R. G., Ruiz-Lapuente, P., Walton, N., Schaefer, B., Boyle, B. J., Filippenko, A. V., Matheson, T., Fruchter, A. S., Panagia, N., Newberg, H. J. M., Couch, W. J., & The Supernova Cosmology Project. 1999, ApJ, 517, 565

Phillips, M. M. 1993, ApJ, 413, L105

Poznanski, D., Chornock, R., Nugent, P. E., Bloom, J. S., Filippenko, A. V., Ganeshalingam, M., Leonard, D. C., Li, W., & Thomas, R. C. 2010, Science, 327, 58

Provencal, J. L., Shipman, H. L., Hog, E., & Thejll, P. 1998, ApJ, 494, 759

Riess, A. G., Filippenko, A. V., Challis, P., Clocchiatti, A., Diercks, A., Garnavich, P. M., Gilliland, R. L., Hogan, C. J., Jha, S., Kirshner, R. P., Leibundgut, B., Phillips, M. M., Reiss, D., Schmidt, B. P., Schommer, R. A., Smith, R. C., Spyromilio, J., Stubbs, C., Suntzeff, N. B., & Tonry, J. 1998, AJ, 116, 1009

Röpke, F. K., Woosley, S. E., & Hillebrandt, W. 2007, ApJ, 660, 1344

Seitenzahl, I. R., Meakin, C. A., Townsley, D. M., Lamb, D. Q., & Truran, J. W. 2009a, ApJ, 696, 515

Seitenzahl, I. R., Townsley, D. M., Peng, F., & Truran, J. W. 2009b, Atomic Data and Nuclear Data Tables, 95, 96

Timmes, F. X. & Swesty, F. D. 2000, ApJS, 126, 501

Townsley, D. M., Calder, A. C., Asida, S. M., Seitenzahl, I. R., Peng, F., Vladimirova, N., Lamb, D. Q., & Truran, J. W. 2007, ApJ, 668, 1118

Valenti, S., Pastorello, A., Cappellaro, E., Benetti, S., Mazzali, P., Manteca, J., Taubenberger, S., Elias-Rosa, N., Ferrando, R., Harutyunyan, A., Hentunen, V.-P., Nissinen, M., Pian, E., Turatto, M., Zampieri, L., & Smartt, S. J. 2009, ArXiv, 0901.2074

Zingale, M., Almgren, A. S., Bell, J. B., Nonaka, A., & Woosley, S. E. 2009, ApJ, 704, 196

Zingale, M., Nonaka, A., Almgren, A. S., Bell, J. B., Malone, C. M., & Woosley, S. E. 2011, ApJ, 740, 8